Excitation transfer between optically injected microdisk lasers

Thomas Van Vaerenbergh,[1,3,*] **Koen Alexander,**[1,3]
Joni Dambre,[2] **and Peter Bienstman**[1,3]

[1]*Photonics Research Group (INTEC), Ghent University - imec, Sint-Pietersnieuwstraat 41, B-9000 Ghent, Belgium*
[2]*Electronics and Information Systems (ELIS), Ghent University, Sint-Pietersnieuwstraat 41, B-9000 Ghent, Belgium*
[3]*Center for Nano- and Biophotonics (NB-Photonics), Ghent University, Sint-Pietersnieuwstraat 41, B-9000 Ghent, Belgium*
[*]*thomas.vanvaerenbergh@intec.ugent.be*

Abstract: Recently, we have theoretically demonstrated that optically injected microdisk lasers can be tuned in a class I excitable regime, where they are sensitive to both inhibitory and excitatory external input pulses. In this paper, we propose, using simulations, a topology that allows the disks to react on excitations from other disks. Phase tuning of the intermediate connections allows to control the disk response. Additionally, we investigate the sensitivity of the disk circuit to deviations in driving current and locking signal wavelength detuning. Using state-of-the-art fabrication techniques for microdisk laser, the standard deviation of the lasing wavelength is still about one order of magnitude too large. Therefore, compensation techniques, such as wavelength tuning by heating, are necessary.

OCIS codes: (200.4700) Optical neural systems; (130.4310) Nonlinear; (140.5960) Semiconductor lasers; (230.1150) All-optical devices

References and links

1. W. Maass, "Networks of spiking neurons: the third generation of neural network models," Neural Networks **10**, 1659–1671 (1997).
2. S. Beri, L. Mashall, L. Gelens, G. Van der Sande, G. Mezosi, M. Sorel, J. Danckaert, and G. Verschaffelt, "Excitability in optical systems close to Z2-symmetry," Phys. Lett. A **374**, 739–743 (2010).
3. W. Coomans, L. Gelens, S. Beri, J. Danckaert, and G. Van der Sande, "Solitary and coupled semiconductor ring lasers as optical spiking neurons," Phys. Rev. E **84**, 036209 (2011).
4. S. Wieczorek, B. Krauskopf, and D. Lenstra, "Multipulse excitability in a semiconductor laser with optical injection," Phys. Rev. Lett. **88**, 063901 (2002).
5. D. Goulding, S. Hegarty, O. Rasskazov, S. Melnik, M. Hartnett, G. Greene, J. McInerney, D. Rachinskii, and G. Huyet, "Excitability in a quantum dot semiconductor laser with optical injection," Phys. Rev. Lett. **98**, 153903 (2007).
6. A. Hurtado, K. Schires, I. D. Henning, and M. J. Adams, "Investigation of vertical cavity surface emitting laser dynamics for neuromorphic photonic systems," Appl. Phys. Lett. **100**, 103703 (2012).
7. S. Barbay, R. Kuszelewicz, and A. M. Yacomotti, "Excitability in a semiconductor laser with saturable absorber," Opt. Lett. **36**, 4476–4478 (2011).
8. M. Brunstein, A. M. Yacomotti, I. Sagnes, F. Raineri, L. Bigot, and A. Levenson, "Excitability and self-pulsing in a photonic crystal nanocavity," Phys. Rev. A **85**, 031803 (2012).
9. A. M. Yacomotti, P. Monnier, F. Raineri, B. Ben Bakir, C. Seassal, R. Raj, and J. A. Levenson, "Fast thermo-optical excitability in a two-dimensional photonic crystal," Phys. Rev. Lett. **97**, 143904 (2006).
10. T. Van Vaerenbergh, M. Fiers, P. Mechet, T. Spuesens, R. Kumar, G. Morthier, B. Schrauwen, J. Dambre, and P. Bienstman, "Cascadable excitability in microrings," Opt. Express **20**, 20292–20308 (2012).

#198417 - $15.00 USD Received 26 Sep 2013; revised 3 Nov 2013; accepted 6 Nov 2013; published 15 Nov 2013

11. M. A. Nahmias, B. J. Shastri, A. N. Tait, S. Member, and P. R. Prucnal, "A leaky integrate-and-fire laser neuron for ultrafast cognitive computing," IEEE J. Sel. Top. Quantum Electron. **16**, 1–12 (2013).
12. J. Van Campenhout, P. Romeo, D. Van Thourhout, C. Seassal, P. Regreny, L. Di Cioccio, J.-M. Fedeli, and R. Baets, "Design and optimization of electrically injected InP-based microdisk lasers integrated on and coupled to a SOI waveguide circuit," J. Lightwave Technol. **26**, 52–63 (2008).
13. Y. De Koninck, K. Huybrechts, G. Van der Sande, J. Danckaert, R. Baets, and G. Morthier, "Nonlinear dynamics of asymmetrically coupled microdisk lasers," in *LEOS Annual Meeting Conference Proceedings, 2009. LEOS'09. IEEE* (IEEE, 2009), pp. 503–504.
14. K. Alexander, T. Van Vaerenbergh, M. Fiers, P. Mechet, J. Dambre, and P. Bienstman, "Excitability in optically injected microdisk lasers with phase controlled excitatory and inhibitory response," Opt. Express **21**, 20292–20308 (2013).
15. M. Turconi, B. Garbin, M. Feyereisen, M. Giudici, and S. Barland, "Control of excitable pulses in an injection-locked semiconductor laser," Phys. Rev. E **88**, 022923 (2013).
16. E. M. Izhikevich, *Dynamical Systems in Neuroscience: The Geometry of Excitability and Bursting (Computational Neuroscience)*, 1st ed. (MIT, 2006).
17. M. Fiers, T. Van Vaerenbergh, K. Caluwaerts, D. Vande Ginste, B. Schrauwen, J. Dambre, and P. Bienstman, "Time-domain and frequency-domain modeling of nonlinear optical components at the circuit-level using a node-based approach," J. Opt. Soc. Am. B **29**, 896–900 (2012).
18. W. Coomans, G. Van der Sande, and L. Gelens "Oscillations and multistability in two semiconductor ring lasers coupled by a single waveguide," Phys. Rev. A **88**, 033813 (2013).
19. P. Mechet, F. Raineri, A. Bazin, Y. Halioua, T. Spuesens, T. Karle, P. Regreny, P. Monnier, D. Van Thourhout, I. Sagnes, R. Raj, G. Roelkens, and G. Morthier, "Uniformity of the lasing wavelength of heterogeneously integrated inp microdisk lasers on soi," Opt. Express **21**, 10622–10631 (2013).
20. L. Liu, T. Spuesens, G. Roelkens, D. Van Thourhout, P. Regreny, and P. Rojo-Romeo, "A thermally tunable iii–v compound semiconductor microdisk laser integrated on silicon-on-insulator circuits," IEEE Photonics Technol. Lett., IEEE **22**, 1270–1272 (2010).

1. Introduction

In Spiking Neural Networks (SNNs), information is processed by excitable neurons, that communicate with each other using pulses. Theoretically, they outperform the computational power of non-spiking artificial neural network types [1]. Given the natural appearance of excitability in many different non-linear optical components, both lasing [2–7] and non-lasing [8–10], there is an intrinsic advantage of implementing such networks in photonic hardware as this would allow to operate at time-scales that are orders of magnitude faster than typical biological and electronic implementations [11].

In this article, microdisk lasers are being proposed as a basic building block for an integrated photonic SNN platform. We elucidate the pulse transfer mechanism between the disks. The microdisk laser consists of a disk-shaped InP laser cavity, bonded on top of a Silicon-On-Insulator (SOI) substrate, supporting two counterpropagating whispering gallery modes [12]. The modes are evanescently coupled to a silicon waveguide in the SiO_2-substrate layer. The evolution of the slowly varying complex field amplitudes of the modes can be described by the rate equations discussed in [13, 14].

For relatively large currents, microdisk lasers tend to lase unidirectionally, and input pulses can switch the lasing direction [13]. By breaking the symmetry of the system, the laser can be made excitable. One way of doing this, as demonstrated in equivalently behaving Semiconductor Ring Lasers (SRLs) [3], is by inducing asymmetry in the intermodal coupling. However, we have recently proposed to use optical injection for this goal, creating a dominating mode (E^+) and a suppressed mode (E^-) [14]. Similar to optically injected single-mode semiconductor lasers [4, 5, 15], this gives rise, in the vicinity of a *Saddle-Node on an Invariant Circle (SNIC)* bifurcation, to class I excitability, which phenomenologically resembles the well-known leaky integrate-and-fire model of a spiking neuron [16]. Small pulses, preferably out of phase with the locking signal, can be used to perturb the laser state, pushing it across this bifurcation. By controlling the phase, both an excitatory and an inhibitory response can be created. Indeed, the importance of the phase of the trigger pulse was recently demonstrated experimentally in

#198417 - $15.00 USD Received 26 Sep 2013; revised 3 Nov 2013; accepted 6 Nov 2013; published 15 Nov 2013

a single-mode semiconductor laser under optical injection [15]. One clear characteristic of the microdisk excitability is that every downward pulse in the dominant mode is accompanied by an upward pulse in the suppressed mode, of approximately the same absolute strength. It is the upwards pulse we will use to excite other disks.

The rest of this paper is structured as follows. Using the same 'neuron' topology and model parameters proposed in our previous paper [14], which exploits the class I excitability mechanism of a microdisk, and by connecting two of these neurons in the topology defined in section 2, we will demonstrate in section 3 cascadability of the excitation mechanism, as this topology allows one disk to trigger an excitation in the second disk. In sections 4 and 5, the sensitivity of this cascade of two disks to variations in laser frequencies and current deviations, respectively, will be discussed. Simulations are done using Caphe, a nonlinear circuit simulator developed in our group [17].

2. Connection topology

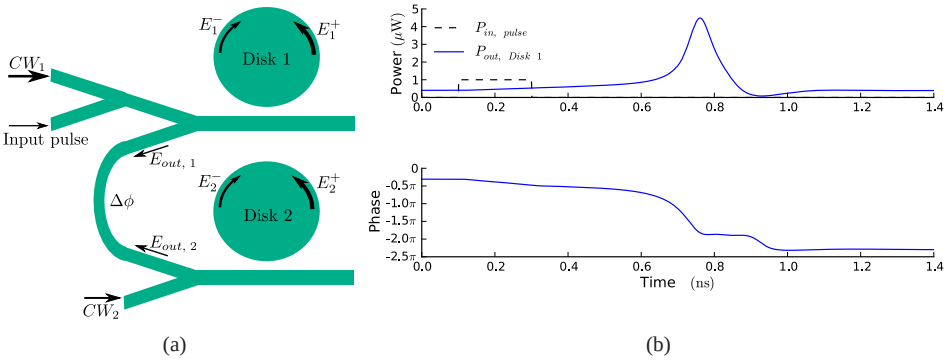

Fig. 1. (a) Topology used to cascade two microdisks. The connection between both lasers imposes a phase difference $\Delta\phi$. (b) Input and output power of the first disk when the second disk is 'turned off' (current as well as locking signal are absent). The bottom graph shows the phase difference between the output pulse and the locking signal.

Figure 1(a) shows the topology of two connected microdisk lasers that is considered throughout this paper. Both microdisk lasers are assumed to be identical, unless mentioned otherwise. Both lasers are locked in the unidirectional regime, close to the saddle-node bifurcation along which excitability was demonstrated in [14]. All splitters in the geometry have a 50/50 splitting ratio. The effective locking signals for the lasers thus carry a quarter of the CW_1-power (P_{CW_1}) and half of the CW_2-power (P_{CW_2}), for disks 1 and 2, respectively. Note as well that the input pulse power is attenuated by a factor of four, before it is felt by disk 1. If the first disk gets excited, its output pulse will travel through the connecting waveguide to the second disk and also this pulse's power will get attenuated by a factor of four. Despite this power loss, due to the strong coupling between the disks and their bus waveguide, the coupling between the two different disks is still $1.8\times$ stronger than the intermodal coupling. To increase the possibility that the output from the first disk excites the second one, the detuning of the locking signal is slightly different in this paper compared to [14] ($\Delta\omega = \omega_{in} - \omega_{disk\,1,2} = -20$ ns^{-1} instead of -15 ns^{-1}). The current is still 2.3 mA. For these parameters, the saddle-node bifurcation lies at $|E_{in}| = 3.63\ \sqrt{\mu \mathrm{W}}$. Additional details about the simulation model and its parameters are summarized in Appendix A and B, respectively.

#198417 - $15.00 USD Received 26 Sep 2013; revised 3 Nov 2013; accepted 6 Nov 2013; published 15 Nov 2013

From the simulations in [14], it is clear that the input pulse is preferably out of phase with the CW locking signal to excite a disk. The phase delay $\Delta\phi$, and the relative phase of both locking signals, will thus be decisive in whether or not the first disk will be able to excite the second one. Moreover, the phase of the output pulse of the first disk is not constant as a function of time. To assure that the first pulse can excite the second one, the phase delay $\Delta\phi$ has to be chosen in such a way that the pulse is out of phase with the CW_2 input, for a significantly long amount of time. We first assume that the two locking signals, CW_1 and CW_2, arrive at the disks having the same phase. Figure 1(b) shows a power and phase trace of the output pulse of first disk (locked with a 3.7 $\sqrt{\mu W}$ locking signal). In Fig. 1(b), one can clearly see that, although the phase of the mode sweeps through the whole 2π-interval, it stays nearly constant during the whole downward stroke of the pulse (around $-1.9\,\pi$). This pulse has to be out of phase with the locking signal at the second disk. This leads to $(2n+1)\pi = -1.9\,\pi + \Delta\phi$, $n \in \mathbb{Z}$, for $n = -1$: $\Delta\phi = 1.9\,\pi - \pi \approx 2.8$ rad.

The transfer of an excitation between excitable lasers is currently only theoretically demonstrated in the case of two SRLs with an asymmetric intermodal coupling [3]. In the latter case, not only a different excitation mechanism is used, but also the asymmetry in the intermodal coupling is chosen such that the SRL that is triggered by an external pulse receives the strong mode from the subsequent SRL, while it sends out its suppressed mode to this other SRL. In contrast, in the topology we currently propose the two disks receive each other's suppressed mode. Indeed, from the viewpoint of the interconnecting waveguide the two disks lase in the symmetric outward state S_{out}, as defined in [18] for two SRLs, interconnected by a single bus waveguide, without optical injection.

3. Transfer of the excitation

In this section, we investigate the transfer of excitations in the proposed topology. First, we study the purely symmetric case of two identical disks driven by an equal locking signal, which results in a continuous transfer of the excitation between the two disks. Next, we induce asymmetry in the system to make the excitation transfer unidirectional.

3.1. Symmetrical coupling: oscillations

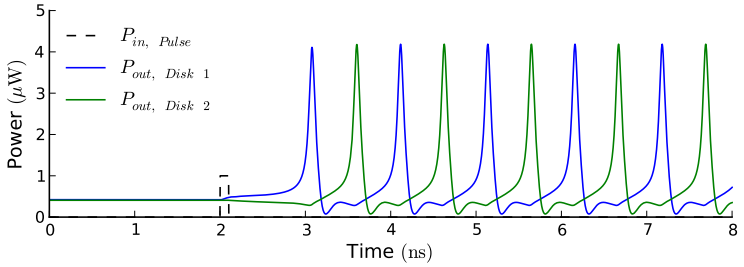

Fig. 2. Input pulse power and output power of both disks. Both disks are pumped with a 2.3 mA current and $\Delta\phi = 2.8$ rad. The locking signals for both disks are 3.8 $\sqrt{\mu W}$. The input pulse is 1 $\sqrt{\mu W}$ strong and 0.1 ns long.

In Fig. 2, time traces of the output power of both disks are shown. Both disks are identically biased. From the trace, it is clear that an excitation of the first disk can travel through the connecting waveguide and in its turn excite the second disk. Apart from the input waveguide for the initial perturbation, the system is purely symmetric. The second disk will therefore in its

#198417 - $15.00 USD Received 26 Sep 2013; revised 3 Nov 2013; accepted 6 Nov 2013; published 15 Nov 2013

turn excite the first one, forming a repeating cycle. This system is in a sense bistable: apart from the initial situation, where the output powers are constant, there exists a limit cycle (LC) of alternating excitations.

Interestingly, in two SRLs without optical injection (but with symmetrical intermodal coupling), coupled through a single bus waveguide, dependent on the phase and strength of the optically coupling, relaxation oscillations that were not present in the individual SRLs can appear in the outward symmetric state S_{out} [18]. However, although a detailed bifurcation analysis still needs to be done, the similarity in pulse shape between Figs. 2 and 1(b), combined with the choice for $\Delta\phi$ needed to obtain this LC, makes it acceptable that the oscillation in the case of coupled optically injected disks is not just a mere consequence of the optical coupling but is also related to the SNIC bifurcation that appears in the individual optically injected disks. The success of the proposals to create a unidirectional excitation transfer in the subsequent paragraph strengthen this hypothesis.

3.2. Asymmetrical coupling: unidirectional excitation transfer

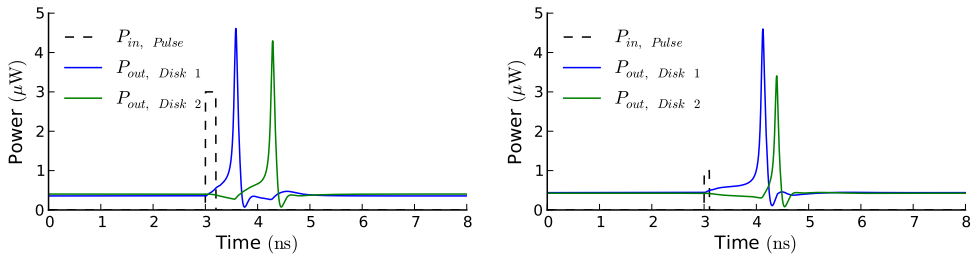

Fig. 3. (a) Symmetry breaking by difference in locking amplitude. The locking signal for the first disk has an amplitude of 4 $\sqrt{\mu\mathrm{W}}$. For the second disk, the locking amplitude is 3.9 $\sqrt{\mu\mathrm{W}}$. Both disks are pumped with a 2.3 mA current, $\Delta\phi = 2.8$ rad. The input pulse is 3 μW strong and 0.2 ns long. (b) Symmetry breaking by difference in locking phase. The locking signals for both disks have an amplitude of 3.55 $\sqrt{\mu\mathrm{W}}$, while $\phi_{CW_2} = \phi_{CW_1} + \frac{\pi}{2}$. Both disks are pumped with a 2.3 mA current, $\Delta\phi = 4.2$ rad. The input pulse is 1 μW strong and 0.1 ns long.

In many cases, the first neuron has to excite the second one, but not the other way round. To obtain this, the symmetry in the system displayed in Fig. 1(a) has to be broken somehow. As a matter of fact, a practical realization of this system will never be purely symmetrical. Parameters of the disks, currents, external reflections, the phase difference between the locking signals, etc. will inevitably create a big asymmetry. However, a deterministically induced asymmetry is preferable. Starting from the simulation in Fig. 2, we propose two distinct ways of breaking the symmetry, in a controlled way. As a first method, one can artificially increase the threshold of the first disk, such that the pulse from the first disk is able to excite the second disk, whereas the (similar) pulse travelling back, is not strong enough to excite the first disk again. Externally, the threshold of a disk can be tuned by either changing its current, or the amplitude of its locking signal. Decreasing the current or increasing the locking amplitude, will increase the threshold. This strategy is demonstrated in Fig. 3(a), where the threshold of disk 1 is larger than the threshold of disk 2 due to an asymmetry in the locking amplitudes. It is clear that the output pulse of the first disk excites the second one, whereas the first disk is not excited by the return-

#198417 - $15.00 USD Received 26 Sep 2013; revised 3 Nov 2013; accepted 6 Nov 2013; published 15 Nov 2013

ing (green) pulse. A clear disadvantage of this strategy is that a stronger input pulse is needed to excite the first disk, since its threshold was artificially increased. In this particular example, the original perturbation carries 6 times more energy than the one used in Fig. 2. This energy problem limits the applicability of this approach to larger circuits of interconnected microdisk lasers.

A second approach to deterministically break the symmetry of the system simulated in Fig. 2, is by inducing a phase difference between the locking signals. For example, both locking signals can be assumed to be in quadrature ($\phi_{CW_2} = \phi_{CW_1} + \frac{\pi}{2}$). The optimal phase delay to transfer the excitation from disk 1 to disk 2 will then increase by $\frac{\pi}{2}$, whereas the optimal delay for transfer of excitation in the opposite direction decreases by $\frac{\pi}{2}$. It is clear that the phase delay can be chosen such that the pulses travelling from disk 1 have an excitatory effect on disk 2, while output pulses from disk 2 have an inhibitory effect on disk one.

In Fig. 3(b), the phase difference between both CW locking signals is $\frac{\pi}{2}$ and $\Delta\phi = 1.9\pi - \frac{\pi}{2} \approx 4.2$ rad. It is clear that the lasers can now be brought in a regime where a relatively weak pulse can excite the first disk, the first disk in its turn excites the second one, but the excitation does not propagate back to the first disk. Note that, due to the change of the connecting waveguide phase delay, the locking amplitude has to be changed compared to the case of Fig. 3(a). Indeed, the small constant signal from one disk interferes differently with the constant locking signal of the other. A clear advantage of this approach is that the threshold of the first disk is not artificially increased.

4. Sensitivity to parameter variations

In this section, we investigate the sensitivity of the response of the topology introduced in section 1(a), starting from the parameters used in Fig. 3(b), to certain parameter variations. In particular, we analyze the sensitivity to current variations and variations of the frequency detuning. Estimates of the robustness to current variations give an idea of how easily this behavior can deal with experimental current fluctuations. Investigating the frequency detuning gives a rough estimate of how well variations in the lasing wavelengths between different disks, as well as the locking signal wavelength, can be tolerated. The exact lasing wavelength can be seen as a net result of other parameter variations, and is experimentally easier to access.

4.1. Influence of current variations

Figure 4 shows the behavior of both disks, for currents $2.3\,\mathrm{mA} + \Delta I_1$ and $2.3\,\mathrm{mA} + \Delta I_2$ through disk 1 and 2, respectively. Black regions represent the single excitation of the disk, in the white regions, the laser does not get excited, neither does it oscillate. The light grey regions give the parameters for which the laser oscillates permanently. In the dark grey regions, the laser shows more complex multipulse excitability, in which the first disk excites multiple times before it is able to excite the second disk and the system finally decays back to the initial condition. The region for which excitability in both disks exists is rather small, with a cross-section of about 0.1 mA. However, a current stability of 0.1 mA is experimentally achievable, such that the current stability will not be the limiting factor in practice. This sensitivity to current variations can be used to make rough estimates of sensitivity to variations in other parameters. Taking into account that the bifurcation locking amplitude at $\Delta\omega = -20\,\mathrm{ns}^{-1}$ changes roughly $1\ \sqrt{\mu\mathrm{W}}$ per mA , a sensitivity to current variations of 0.1 mA corresponds to a sensitivity to roughly $0.1\ \sqrt{\mu\mathrm{W}}$ of locking amplitude variation.

Since, above lasing threshold, the output power of a laser increases linearly with the current, the saddle-node bifurcation shifts to higher injection amplitudes when the current increases, i.e., the input power needed to lock the laser has to increase with increasing driving current. This explains the general behavior of the two disks in Fig. 4. Indeed, for a single disk and at low

#198417 - $15.00 USD Received 26 Sep 2013; revised 3 Nov 2013; accepted 6 Nov 2013; published 15 Nov 2013

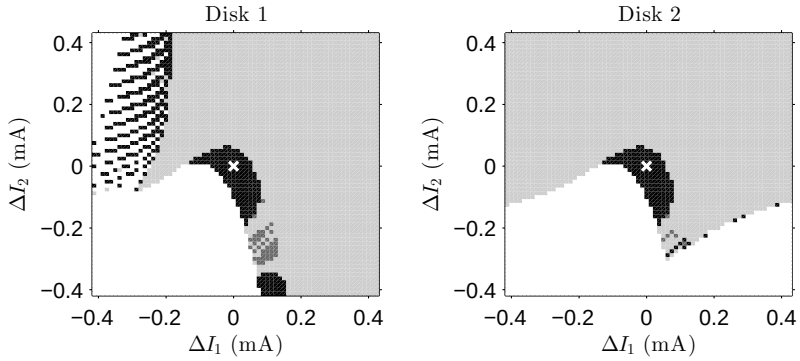

Fig. 4. Influence of variations of the current through disks 1 and 2, ΔI_1 and ΔI_2, respectively. Unperturbed, both currents are 2.3 mA, $\Delta\phi = 4.2$ rad. The locking signals for both disks are 3.55 $\sqrt{\mu\text{W}}$ and the input pulse is 1 μW strong and 0.15 ns long. As we are interested in an unidirectional excitation transfer, the optimal current setting appears when both disks only excite once. We represent a single excitation of the respective disk using black pixels, so the cross section of the black regions in both plots defines the domain with a unidirectional excitation transfer. In the light grey regions, the disk output is oscillating, independent of the perturbation. In the white regions, there is neither oscillation, nor excitation. In the dark grey regions, the disk shows more complex multipulse excitability (two pulses or more, after which the system decays again). The white cross represents the unperturbed system ($\Delta I_1 = 0$ and $\Delta I_2 = 0$).

currents, the bifurcation lies far below the amplitude of the locking signal, and the pulses are too weak to excite the laser. When the current is increased, the locking amplitude at the saddle-node bifurcation approaches the current locking amplitude and excitation becomes possible. However, when the current is increased even more, the bifurcation locking amplitude ends up above the locking amplitude, and the mode power oscillates. In Fig. 4, the same principle is reflected in the behavior of the coupled disks: for each of the lasers, one can typically find oscillating regimes in higher current regions, unresponsive regions at lower currents and more complex behavior, such as excitation, in between. Due to the coupling between the lasers, the diagrams are not as 'clean' as could be expected: more complex dynamic regimes appear that are less easy to interpret. For instance, in the region in the upper left corner, the second disk oscillates, whereas the first disk gets either excited, or not. Indeed, the locking signal of the first disk is produced by interference between the oscillating output of the second disk and a CW locking signal. In this region, the first disk will either get excited, or not, depending on the timing of the pulse within the oscillation period of the second disk.

Another consequence of the current dependence of the bifurcation locking amplitude is that Fig. 4 depends on the strength of the input pulses, as the excitation threshold gradually increases when moving away towards lower currents. Consequently, at currents for which weak pulses are not capable of exciting the first disk, excitation can become possible when using stronger pulses, possibly inducing a response of the second disk.

4.2. Influence of detuning variations

When producing several disks, there will be a certain variation on the exact laser wavelength. Therefore, if one connects two lasers, there will be a certain deviation on the detuning with respect to the locking signals. Figure 5 shows how a deviation in detuning can change the behavior demonstrated in Fig. 3(b). The general trends are similar to those observed for current

#198417 - $15.00 USD Received 26 Sep 2013; revised 3 Nov 2013; accepted 6 Nov 2013; published 15 Nov 2013

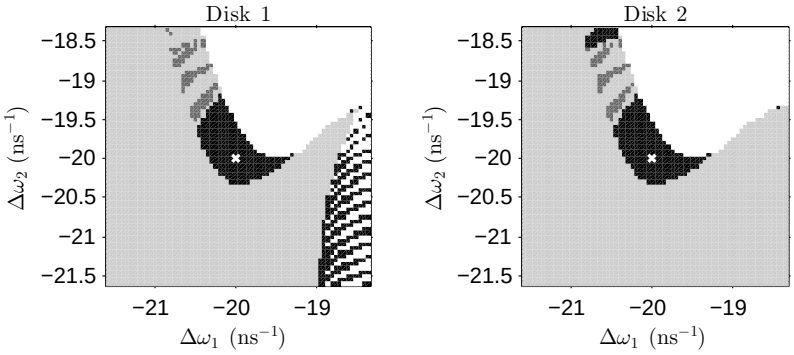

Fig. 5. Influence of variations of the frequency detunings of both disks, $\Delta\omega_1$ and $\Delta\omega_2$, respectively. Unperturbed, the detuning is -20 ns^{-1}. The locking amplitude for both disks is 3.55 $\sqrt{\mu\text{W}}$. The input pulse is 1 μW strong and 0.15 ns long. The colors represent the same behaviors as in Fig. 4.

deviations. For a single disk, the locking amplitude of the saddle-node bifurcation decreases when the detuning $\Delta\omega$ approaches zero [14]. Hence, bringer $\Delta\omega$ closer to 0 has an effect similar to decreasing current. One can clearly see that Fig. 5 has a similar structure as Fig. 4, but mirrored around the center. Figure 5 shows that the excitability is very sensitive to deviations of the detuning. Roughly, the excitability can be found in a region of about 1 ns^{-1} wide, which corresponds to ~ 1.27 pm in wavelength, whereas variations larger than a picometer already cause completely different behavior. Unfortunately, using current fabrication techniques, the typical variations in microdisk laser wavelength, are on the order of 0.4 nm [19]. Consequently, it is important to know how to deal with those wavelength fabrications. For this reason, we will discuss some compensation techniques in the next section.

5. Compensating for variations in detuning

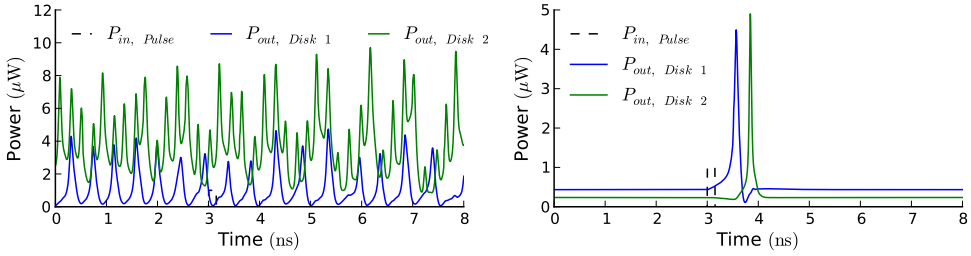

Fig. 6. (a) Time trace of output powers of both lasers, the detuning of the second laser is now -40 ns^{-1}, other parameters are identical to the ones used in Fig. 3(b). (b) Time trace of output powers of both lasers, the detuning of the second laser is still -40 ns^{-1}, I_2 is decreased to 1.7 mA. The locking signal amplitudes are 3.55 $\sqrt{\mu\text{W}}$ and $\sqrt{3}\cdot 3.55$ $\sqrt{\mu\text{W}}$, for disk 1 and 2, respectively.

At first sight, the excitable behavior, and the transfer of excitability between two disks, as

#198417 - $15.00 USD Received 26 Sep 2013; revised 3 Nov 2013; accepted 6 Nov 2013; published 15 Nov 2013

presented in section 3 and 4, is extremely sensitive to process variations. However, for the simulations presented in section 4, either currents, or detunings were swept, while keeping all other parameters the same. It is possible to compensate for a change in wavelength by changing other parameters. As an example, we illustrate how a $-20\,\mathrm{ns}^{-1}$ detuning mismatch of the second disk with respect to the first disk (i.e., $\Delta\lambda_2 = 51$ pm instead of $\Delta\lambda_1 = 25.5$ pm) can be compensated. Figure 6(a) shows how, without any compensation for this mismatch, both lasers exhibit complex self-pulsating behavior instead of the desired unidirectional pulse transfer. The reason for this complex behavior is that, for this wavelength detuning, the threshold value to obtain locking, which is also related to the SNIC bifurcation used for the excitation process, lies far above the current locking amplitude for the second laser. To see the same kind of behavior, the microdisk can be either locked using a higher amplitude, or the current can be lowered such that the bifurcation value is artificially decreased. In Fig. 6(b), the desired behavior (transfer of excitation from disk 1 to disk 2) is restored by using a combination of both strategies. The current through the second disk is decreased to 1.7 mA, and the locking power is tripled.

Using current and locking power to correct for deviations in lasing frequency, the fabrication tolerances can be relaxed with roughly a factor of 10 (a few tens of pm). This is still insufficient in view of what current fabrication techniques can achieve. Other strategies, such as deliberately changing the lasing wavelength using thermo-optic effects, can be considered. In [20], it is shown that with appropriately designed heaters, the lasing wavelength of microdisk lasers can be changed over a range of about 2 nm.

6. Conclusion

In this paper, cascadability of the neuron topology introduced in our previous paper [14] was demonstrated. The choice of the phase delay in the waveguide interconnection crucially determines its excitatory (inhibitory) character by forcing destructive (constructive) interference of the output pulse of the sending disk with the locking signal of the receiving disk. When simulating a perfectly symmetrical pair of coupled disks, with a phase that corresponds to an excitatory connection, alternate oscillations going back and forth between the neurons appear. To avoid this oscillating behavior, the symmetry of the system can be broken, either by naively increasing the excitation threshold of one of the disks, or by inducing a phase difference between the locking signals of both lasers. For both methods, the lasers can be brought in a regime where only unidirectional transfer of excitation occurs. The latter behavior roughly gets lost for current variations of 0.1 mA, and frequency variations on the order of $1\,\mathrm{ns}^{-1}$ (≈ 1.27 pm). One can however compensate for detuning variations by changing other, more controllable, parameters, such as the locking amplitude or the current, making the transfer of excitation robust to variations in lasing wavelength of several tens of pm. However, using the state-of-the-art production techniques for microdisk lasers, the standard deviation of the lasing wavelength is still about one order of magnitude larger. Additional compensation techniques, such as wavelength tuning by heating, will have to be considered.

Appendices

A. Rate equation model of two coupled microdisk lasers

A single microdisk laser can be described in the slowly varying amplitude approach using the coupled rate equations mentioned in [14], representing the evolution of the complex mode amplitudes, E^+ and E^- ($|E_\pm|^2$ is the number of photons in the mode, while the optical field oscillates with an additional $e^{-j\omega_{int}t}$-dependency), and the number of free carriers, N, in the cavity. Caphe, the circuit simulator we use in this paper, converts the equations that describe the coupling of the optical modes to the bus waveguide into the formalism described in [17],

#198417 - $15.00 USD Received 26 Sep 2013; revised 3 Nov 2013; accepted 6 Nov 2013; published 15 Nov 2013

which, for the topology proposed in Fig. 1(a), results in the following set of coupled differential equations:

$$\begin{aligned}
\frac{dE_1^+}{dt} &= \frac{1}{2}(1-j\alpha)\left(G_1^+ - \frac{1}{\tau_p}\right)E_1^+ + j\Delta\omega_1 E_1^+ + CE_1^- \\
&\quad -j\frac{\kappa\sqrt{\tau}}{\sqrt{\hbar\omega_0}}\left[-j\kappa\sqrt{\hbar\omega_0\tau}\frac{1}{\sqrt{2}}\left(e^{j\Delta\phi}\frac{1}{\sqrt{2}}E_2^-\right)+\frac{1}{\sqrt{2}}\left(\frac{1}{\sqrt{2}}E_{CW,1}+\frac{1}{\sqrt{2}}E_{tr}\right)\right], \quad (1)\\
\frac{dE_1^-}{dt} &= \frac{1}{\sqrt{2}}(1-j\alpha)\left(G_1^- - \frac{1}{\tau_p}\right)E_1^- + j\Delta\omega_1 E_1^- + CE_1^+, \quad (2)\\
\frac{dE_2^+}{dt} &= \frac{1}{2}(1-j\alpha)\left(G_2^+ - \frac{1}{\tau_p}\right)E_2^+ + j\Delta\omega_2 E_2^+ + CE_2^- \\
&\quad -j\frac{\kappa\sqrt{\tau}}{\sqrt{\hbar\omega_0}}\left[-j\kappa\sqrt{\hbar\omega_0\tau}\frac{1}{\sqrt{2}}\left(e^{j\Delta\phi}\frac{1}{\sqrt{2}}E_1^-\right)+\frac{1}{\sqrt{2}}E_{CW,2}\right], \quad (3)\\
\frac{dE_2^-}{dt} &= \frac{1}{\sqrt{2}}(1-j\alpha)\left(G_2^- - \frac{1}{\tau_p}\right)E_2^- + j\Delta\omega_2 E_2^- + CE_2^+, \quad (4)\\
\frac{dN_i}{dt} &= \frac{\eta I_i}{q} - \frac{N_i}{\tau_c} - G_i^+\left|E_i^+\right|^2 - G_i^-\left|E_i^-\right|^2, \quad (5)\\
G_i^\pm &= \frac{\Gamma g_N (N_i - N_0)}{1+\Gamma\varepsilon_{NL}\left(\left|E_i^\pm\right|^2 + 2\left|E_i^\mp\right|^2\right)}. \quad (6)
\end{aligned}$$

In Eqs. (1)–(4), α is the line broadening factor, τ_p the photon lifetime in the cavity, τ is the roundtrip time of the cavity, $\Delta\omega = \omega_{in} - \omega_i$ the detuning between the input light ω_{in} and the free-running cavity frequency ω_i of disk i ($i \in \{1,2\}$, unless otherwise mentioned $\omega_1 = \omega_2 = \omega_0$), C is the complex intermodal coupling coefficient. κ is the coupling between the disks and the waveguide. $E_{CW,i}$ are the complex amplitudes of the optical inputs used for the locking of both disks, while E_{tr} is the complex amplitude of the input pulse (in both cases $|E_\alpha|^2$ is the power in the waveguide). $\Delta\phi$ is the phase difference due to the interconnecting waveguide. The factors $\frac{1}{\sqrt{2}}$ are due to the power loss in the splitters. Equation (5) describes the evolution of the number of free carriers N_i. I_i is the injected current to each disk, q the elementary charge, η a current efficiency factor, and τ_c the carrier lifetime. $G_i^\pm$ are the gain coefficients of the modes, g_N is the differential gain, N_0 the transparency threshold of free carriers and Γ the confinement factor. The denominator in Eq. (5) includes cross- and self-gain modulation, ε_{NL} is called the nonlinear gain suppression coefficient. The complex amplitude of the output of disk i towards the connecting waveguide can be calculated using:

$$E_{out,i} = -j\kappa\sqrt{\hbar\omega_0\tau}e^{j\Delta\phi}\tfrac{1}{\sqrt{2}}E_i^-. \quad (7)$$

Similar to the intermodal coupling C, this results in an intercavity coupling term $K = -\frac{\kappa^2\tau}{2}e^{j\Delta\phi}$, coupling the suppressed mode of a disk to the strong mode of the other disk. Given $\frac{|K|}{|C|} = 1.80 > 1$, the coupling is clearly stronger than the weak coupling regime as used so far for two coupled excitable SRLs with asymmetric intermodal coupling [3].

B. Numerical details of the simulations

Table 1 summarizes the model parameters used in this paper, representing a typical microdisk.

#198417 - $15.00 USD Received 26 Sep 2013; revised 3 Nov 2013; accepted 6 Nov 2013; published 15 Nov 2013

Table 1. Model parameters are taken from [14].

Parameter	Symbol	Value	Unit
Resonance wavelength	$\lambda_0 = \frac{2\pi c}{\omega_0}$	1.55	μm
Line broadening factor	α	3	
Photon lifetime	τ_p	4.17	ps
Radius microdisk	R	5	μm
Cavity roundtrip time	τ	350	fs
Intermodal coupling	C	$0.449 + 2.82j$	GHz
Amplitude coupling to the waveguide	κ	171.4	GHz
Current efficiency	η	0.5	
Group velocity of the mode	v_g	$8.82 \cdot 10^7$	$\frac{\text{m}}{\text{s}}$
Carrier lifetime	τ_c	600	ps
'Effective' differential gain	Γg_N	982.3	kHz
'Effective' nonlinear gain suppression	$\Gamma \varepsilon_{NL}$	$1.96 \cdot 10^{-6}$	
Transparency carrier amount	N_0	763500	

Acknowledgments

This work is supported by the interuniversity attraction pole (IAP) Photonics@be of the Belgian Science Policy Office and the ERC NaResCo Starting grant. T. Van Vaerenbergh is supported by the Flemish Research Foundation (FWO-Vlaanderen) for a PhD Grant.

#198417 - $15.00 USD Received 26 Sep 2013; revised 3 Nov 2013; accepted 6 Nov 2013; published 15 Nov 2013